JOC Article

Crystal Structure and Photochemical Behavior in Solution of the 3′-*N*-Sulfamate Analogue of Thymidylyl(3′-5′)thymidine

Céline Moriou,[†] Martial Thomas,[†] Marie-Thérèse Adeline,[†] Marie-Thérèse Martin,[†] Angèle Chiaroni,[†] Sylvie Pochet,[‡] Jean-Louis Fourrey,[†] Alain Favre,[§] and Pascale Clivio*,[†]

Institut de Chimie des Substances Naturelles, CNRS, 1 Avenue de la Terrasse, 91190 Gif sur Yvette, France, Unité de Chimie Organique, URA 2128, Institut Pasteur, 25 rue du Docteur Roux, 75724 Paris cedex, France, and Laboratoire de Photobiologie Moléculaire, Institut Jacques Monod, CNRS, Universités Paris 6 et Paris 7, 2 Place Jussieu, 75251 Paris cedex 05, France

pascale.clivio@univ-reims.fr

Received July 18, 2006

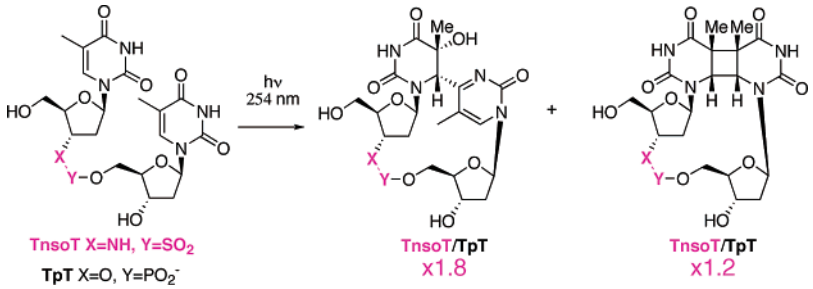

The 3′-*N*-sulfamate analogue of thymidylyl(3′-5′)thymidine (TnsoT, **1**) exhibits a preference for a C3′-endo conformation in the solution and solid states. Its photochemical behavior in solution is compared to that of its natural counterpart, thymidylyl(3′-5′)thymidine (TpT, **2**), to get further insight into the significance of the C3′-endo conformation on the photoproduct formation at the single-stranded dinucleotide level. Irradiation at 254 nm of **1** led to the same type of photoproducts as observed with **2**. However, **1** was significantly more photoreactive than **2**, and accordingly, the initial rate of photoproduct formation was enhanced in accordance with its propensity to base stack compared to **2**. The corresponding quantum yields were determined and showed that the enhancement factor (**1** compared to **2**) is moderate for the cyclobutane pyrimidine dimer (CPD) (1.26) and much higher for the (6-4) photoproduct (1.8). These data strongly suggest that the CPD and (6-4) photoproduct arise from distinct minor stacked conformations.

Introduction

The interplay between DNA conformation and its photochemistry is among the most important issues to address with regard to the respective contribution of each kind of DNA photoproduct (PP) in photoimmune suppression, photocarcinogenesis, apoptosis, or cell-cycle arrest.[1,2] Previous studies performed on the DNA double helix have evidenced two interesting photochemical features at dithymine sites: (1) the formation of the cyclobutane pyrimidine dimer (CPD) is higher in denatured than in native DNA at the same temperature as well as in film and frozen native DNA;[3] and (2) this tendency is reversed for the pyrimidine(6-4)pyrimidone photoproduct ((6-4) PP) formation.[3] Such an observation suggests either that CPD formation requires more conformational freedom than (6-4) PP formation or that the geometry of adjacent thymines in the solid state (generally associated with the A-DNA conformation) is more prone to undergo a Paternó−Büchi reaction (leading to (6-4) formation) than the one achieved in solution. However, recently, CPD formation was shown to be reduced in single- and double-stranded DNA upon a temperature increase whereas (6-4) PP formation was slightly increased.[4] Finally, the A

* Current address: FRE 2715 CNRS, Université de Reims Champagne-Ardenne, 51 rue Cognacq Jay, 51 096 Reims cedex, France.
† Institut de Chimie des Substances Naturelles.
‡ Unité de Chimie Organique, Département de Biologie Structurale et Chimie.
§ Laboratoire de Photobiologie Moléculaire.

(1) (a) Ullrich, S. E. *Front. Biosci.* **2002**, *7*, d684−703. (b) Matsumura, Y.; Ananthaswamy, H. N. *Front. Biosci.* **2002**, *7*, d765−783.

(2) Lo, H.-L.; Nakajima, S.; Ma, L.; Walter, B.; Yasui, A.; Ethell, D. W.; Owen, L. B. *BMC Cancer* **2005**, *5*, 135−142.

(3) Patrick, M. H.; Rahn, R. O. In *Photochemistry and Photobiology of Nucleic Acids: Photochemistry of DNA and Polynucleotides: Photoproducts*; Wang, S. Y., Ed.: Academic Press: New York, 1976; Vol. 2, pp 35−95.

(4) Douki, T. *J. Photochem. Photobiol. B: Biol.* **2006**, *82*, 45−52.

10.1021/jo061488a CCC: $37.00
Published on Web 12/07/2006

conformation of DNA or RNA, which is associated with more nucleobase rigidity, reduces considerably the formation of dithymine photoproducts with respect to the B conformation of DNA.[5] Despite these observations, no precise relationship linking PP formation and DNA conformation has ever been determined. An in-depth understanding of these relationships at the single-stranded dinucleotide level could be helpful to understand the phenomenon occurring at the more complex double-stranded DNA level.

The sugar pucker is one of the major conformational parameters that distinguishes B- from A-DNA.[6a] At the dinucleotide level, the lack of base-pairing and stacking interactions with neighboring bases provides accurate information on the intrinsic puckering effects on the photochemistry. Currently, we investigate the photochemistry of dinucleotide analogues endowed with an A sugar conformation (major C3′-endo puckering) and have recently demonstrated that the 254 nm irradiation of 2′-*O*,5-dimethyluridylyl(3′-5′)-2′-*O*,5-dimethyluridine (TmopTmo), an analogue of thymidylyl(3′-5′)thymidine (TpT, **2**) exhibiting a major C3′-endo conformer population, is qualitatively comparable to that of **2** but significantly faster.[7] These results were rationalized by the increased propensity of the modified dinucleotide to adopt a base-stacked conformation geometry reminiscent of that of TpT.[7]

To probe the generality of this observation, we decided to examine the photochemical behavior of other analogues of TpT possessing a major C3′-endo sugar pucker and an increased base stacking ability compared to **2**. To get deeper insight into the impact of the C3′-endo sugar pucker on the photochemistry, it is crucial to investigate TpT analogues that are not modified at the C2′-position. In this respect, the influence of the modification of the phosphate backbone on the photochemistry looked particularly attractive. The 3′-*N*-sulfamate analogue of thymidylyl(3′-5′)thymidine (TnsoT, **1**), in which the phosphodiester linkage is replaced by a sulfamate group, has been reported to possess the two above conformational criteria in solution.[8] Because the X-ray crystallographic study that we carried out confirmed this propensity, we decided to study its photochemical behavior at 254 nm. We herein report our results and compare them with those of the reference compound TpT (**2**).

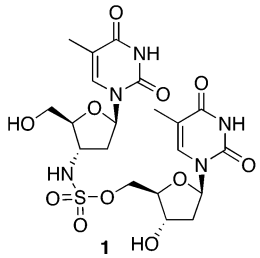

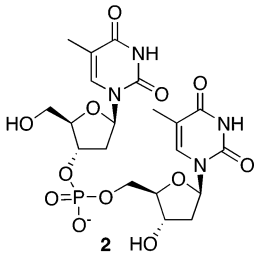

Results

Synthesis of 3′-Deoxythymidin-3′-ylsulfamoyl-[3′(*N*)->5′-(*O*)]-thymidine (1). Compound **1** was prepared following a slightly modified literature procedure (3′-*O*-acetylthymidine **4** was used in place of 3′-*O*-(*tert*-butyldimethylsilyl)thymidine).[8]

SCHEME 1[a]

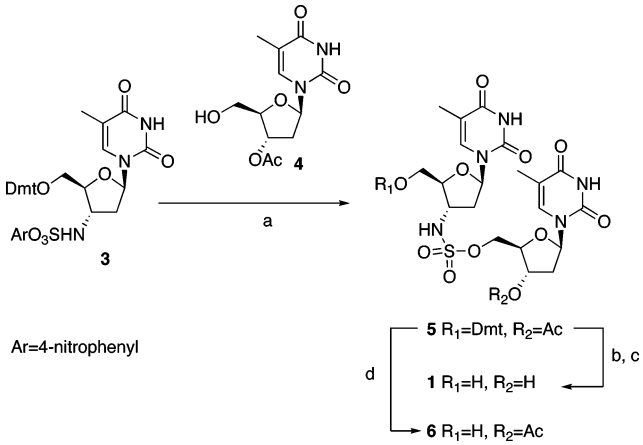

[a] Reagents and conditions: (a) 4 Å molecular sieves, Et_3N, CH_2Cl_2, 68%; (b) MeOH, Et_3N, H_2O (10:1:1); (c) CH_2Cl_2, 80% aq AcOH, 82% (two steps); (d) 3% CF_3COOH, CH_2Cl_2, 92%.

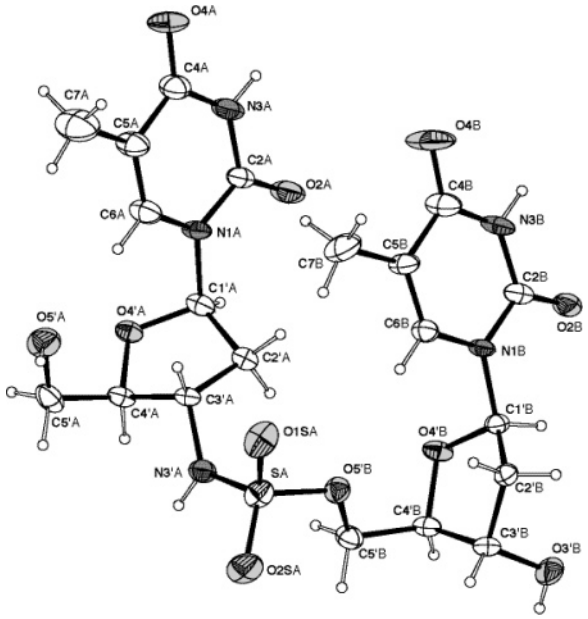

FIGURE 1. ORTEP drawing of the X-ray structure of molecule (AB) **1**.

4-Nitrophenyl 5′-*O*-(4,4′-dimethoxytrityl)-3′-deoxythymidine-3′-sulfamate **3**[8] was reacted with **4** to yield the orthogonally diprotected dimer intermediate **5** (68%). Subsequent deacetylation (MeOH, Et_3N, H_2O) and detritylation (80% aq acetic acid) afforded **1** in 82% yield (Scheme 1).

X-Ray Crystallographic Structure of 1. Upon standing in methanol, slowly occurring transesterification of **6** afforded **1** which crystallized in the chiral space group P1 of the triclinic system, with two independent TnsoT molecules, AB and CD, in the unit cell. One of them, AB, appears in Figure 1, giving the atomic labeling, with the known absolute configuration. These two molecules are hydrogen bonded together through the 3′OH-group of the first molecule (AB) and the C2-oxygen of

(5) (a) Becker, M. M.; Wang, Z. *J. Biol. Chem.* **1989**, *264*, 4163−4167. (b) Kundu, L. M.; Linne, U.; Marahiel, M.; Carell, T. *Chem.−Eur. J.* **2004**, *10*, 5697−5705.

(6) (a) Saenger, W. In *Principles of Nucleic Acid Structure*; Cantor, C. R., Ed.; Springer-Verlag: New York, 1984. (b) Altona, C.; Sundaralingam, M. *J. Am. Chem. Soc.* **1972**, *94*, 8205−8212.

(7) Ostrowski, T.; Maurizot, J.-C.; Adeline, M.-T.; Fourrey, J.-L.; Clivio, P. *J. Org. Chem.* **2003**, *68*, 6502−6510.

(8) (a) Fettes, K. J.; Howard, N.; Hickman, D. T.; Adah, S. A.; Player, M. R.; Torrence, P. F.; Micklefield, J. *Chem. Commun.* **2000**, 765−766. (b) Fettes, K. J.; Howard, N.; Hickman, D. T.; Adah, S.; Player, M. R.; Torrence, P. F.; Micklefield, J. *J. Chem. Soc., Perkin Trans. I* **2002**, 485−495.

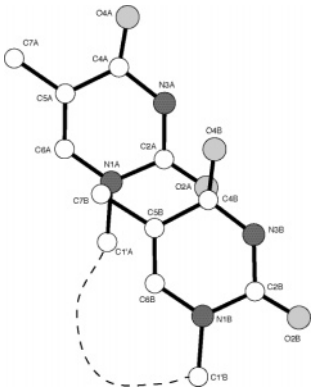

FIGURE 2. View of the geometry of molecule (AB) nucleobases, projected on the A thymine plane.

TABLE 1. Backbone Torsion Angles $\alpha_{(i)}$, $\beta_{(i)}$, $\gamma_{(i)}$, $\delta_{(i)}$, $\epsilon_{(i)}$, and $\zeta_{(i)}$ of the Sugar of Residue i[a] in the X-ray Structure of Molecule (AB) 1

	γ_A	δ_A	ϵ_A	ζ_A	α_B	β_B	γ_B	δ_B
1 (AB)	51.9	81.8	−170.5	−78.2	−60.2	−179.9	62.9	148.9

[a] i = A corresponds to the 5′-residue, and B corresponds to the 3′-residue.

the second one (CD) according to the scheme: O3′B−H···O2C = 3.010(3) Å, H···O2C = 2.35 Å, angle O−H···O = 138.4°. Molecule CD can be fitted on molecule AB by a rotation of 180° around the *a* cell axis direction followed by a translation of 4.117 Å along this axis. The distance between their respective centroids is 8.781 Å. These two molecules display an extremely similar conformation as shown by the root mean square (rms) difference between their atomic coordinates (excluding H atoms) of 0.207 Å, leading to the respective bond and angle rmsd of 0.010 Å and 0.77°. So, only the conformational parameters of molecule AB will be discussed (a complete description of the two molecules is reported in the Supporting Information).[9]

In this molecule (AB), the two thymine bases are in an anti glycosidic bond conformation where χA = −140.1° and χB = −105.7°. The 5′-sugar exhibits a C3′-endo conformation (P = 12.6° and τ_m = 33.6°), whereas the 3′-sugar displays a C2′-endo conformation (P = 179.7° and τ_m = 35.7°).[6] These two bases are nearly parallel as revealed by the dihedral angle of their plane (8.2°). The angle of vectors along the two C5−C6 bonds of 8.75° indicates that the corresponding bonds are nearly parallel. Consequently, no twist exists between the bases, as in A- or B-DNA. The distance Cg(A)−Cg(B) between the ring centroids of the two bases is 5.603(7) Å. With the perpendicular distance of Cg(A) on ring B being 4.020 Å and that of Cg(B) on ring A being 4.388 Å, the two mean planes can be considered distant from 4.204 Å. However, the two thymine bases are not superimposed and only the methyl C7B and the carbon atom C4B nearly overlap with atoms N1A and O2A, leading to a relative gliding of 3.702 Å between the rings, as shown in Figure 2.

The backbone torsion angles are reported in Table 1. The torsion angle ζ (C3′−N−S−O) is in the g- conformation (−78.2°).

Photochemical Behavior of 1. Irradiation of an aqueous solution of **1** at 254 nm led to the formation of two PPs (**7** and **8**) as evidenced by HPLC and ^{1}H NMR analysis of the crude irradiation mixture. Photoproduct **7** showed an UV maximum absorption at 327 nm in accordance with a (6-4) PP structure,[10] whereas photoproduct **8** lacked UV absorbance above 240 nm as expected for a CPD PP. ^{1}H NMR analysis of the crude irradiation mixture confirmed that the two PPs indeed belonged to the (6-4) and CPD PP classes, respectively.[10,11] The presence of two H6 protons at δ 8.08 and 5.22 ppm and of two methyl protons at δ 2.35 and 1.77 ppm in the ^{1}H NMR was the signature of the C5 (*R*) and C6 (*S*) stereochemistry of **7** as observed for **11**, the (6-4) adduct of TpT.[10] In contrast, the stereochemistry of **8** was more ambiguous to assign from the chemical shifts of its two shielded methyl signals (δ 1.59 and 1.48).[11] Therefore, we carried out structural analysis studies to unambiguously establish the stereochemistry of the CPD derived from TnsoT.

Assignment of the Stereochemistry of the Photoproducts. Preparative irradiation was conducted on the 3′-*O*-acetyl derivative **6**, obtained in 92% yield upon TFA treatment of **5** (Scheme 1), to ease the purification step. Irradiation of an aqueous solution of **6** at 254 nm led to the formation of a (6-4) PP **9** and a CPD PP **10** isolated by reversed-phase HPLC in 19 and 10% yield, respectively, together with 28% of recovered **6**. Attribution of the stereochemistry of the asymmetric centers of **10** was performed using 2D NMR techniques. The cis−syn (c,s) stereochemistry of **10** was deduced from the NOEs between H6 Tnso- and H3′ Tnso-, between CH_3 Tnso- and H6 -nsoT, between H6 -nsoT and H2′ -nsoT, and between CH_3 -nsoT and CH_3 Tnso-. NOEs observed for **9** confirmed the C5 (*R*) and C6 (*S*) stereochemistry.

Thus, **9** and **10** arise from cycloaddition reactions between the two thymine bases of **6** in an anti glycosidic bond conformation as in the case of the natural dinucleotide **2**. To demonstrate that the same stereochemical course of the photoreactions had occurred upon irradiation of **1**, we irradiated a mixture of **1** and **6** and observed, upon alkaline treatment (see Experimental Section), the coalescence of the peaks corresponding to the CPD and (6-4) PPs of **6** with those of **1** (photoproducts **7** and **8**). Therefore, the stereochemistry of PPs **7** and **8** is identical to that of PPs **11** and **12** derived from TpT (Scheme 2).

Comparative Photoreactivity of 1 and 2. From the data above, it can be concluded that **1** and **2** generate the same major photoproducts. To closely compare their photochemical behavior, an aqueous equimolar mixture of **1** and **2** was irradiated at 254 nm and the crude irradiation mixture was analyzed by RP HPLC at various times of irradiation (see Supporting Information). As the reactants and photoproducts were well resolved on the HPLC chromatograms, each individual peak (230 nm) could be accurately integrated, yielding the corresponding ΔS_i values. In the following, **1** and **2** will be abbreviated R1 and R2 and their major photoproducts will be abbreviated C1, P1 and C2, P2 (C for CPD and P for (6-4) PP), respectively.

Kinetics of Photoproduct Formation. The fractional amounts Z_{R1} and Z_{R2} of TnsoT (**1**) and TpT (**2**), respectively, at time t of the reaction are given by eq 1

$$Z_{R1} = \frac{\Delta S_{R1}}{\Delta S_{01}} \quad Z_{R2} = \frac{\Delta S_{R2}}{\Delta S_{02}} \tag{1}$$

(9) CCDC 612018 contains the supplementary crystallographic data for this paper. These data can be obtained free of charge at www.ccdc.cam.ac.uk/conts/retrieving.html [or from the Cambridge Crystallographic Data Centre, 12 Union Road, Cambridge CB 1EZ, U.K.; fax/(internat.) +44-1223/336-033; E-mail deposit@ccdc. cam. ac.uk].

(10) Rycyna, R. E.; Alderfer, J. L. *Nucleic Acids Res.* **1985**, *13*, 5949−5963.

(11) Koning, T. M. G.; van Soest, J. J. G.; Kaptein, R. *Eur. J. Biochem.* **1991**, *195*, 29−40.

SCHEME 2

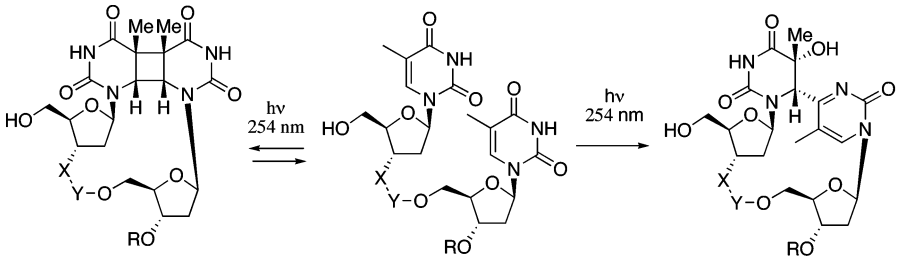

8 X=NH, Y=SO_2, R=H **1** X=NH, Y=SO_2, R=H **7** X=NH, Y=SO_2, R=H

10 X=NH, Y=SO_2, R=$COCH_3$ **6** X=NH, Y=SO_2, R=$COCH_3$ **9** X=NH, Y=SO_2, R=$COCH_3$

12 X=O, Y=PO_2^-, R=H **2** X=O, Y=PO_2^-, R=H **11** X=O, Y=PO_2^-, R=H

TABLE 2. Molar Extinction Coefficient ϵ (M^{-1} cm^{-1}) of TpT and Its Major PPs[a]

	TpT (**2**)	(6−4) PP (**11**)	c,s CPD (**12**)
ϵ_{230}	5300	7300	4000

[a] Derived from Johns et al. data.[12]

where ΔS_{01} (ΔS_{02}) and ΔS_{R1} (ΔS_{R2}) are the peak areas (at 230 nm) corresponding to R1 (R2) at, respectively, time 0 and t of the photoreaction. Practically at $t = 0$, $\Delta S_{01} \approx \Delta S_{02}$.

Similarly, the fractional amounts Z_{C1} and Z_{C2} of the major c,s CPD of **1** and **2** are

$$Z_{C1} = \frac{\Delta S_{C1}}{\Delta S_{01}} \frac{\epsilon_{230}^{R1}}{\epsilon_{230}^{C1}} \quad Z_{C2} = \frac{\Delta S_{C2}}{\Delta S_{02}} \frac{\epsilon_{230}^{R2}}{\epsilon_{230}^{C2}} \tag{2}$$

and the fractional amounts Z_{P1} and Z_{P2} of the (6-4) PP of **1** and **2** are

$$Z_{P1} = \frac{\Delta S_{P1}}{\Delta S_{01}} \frac{\epsilon_{230}^{R1}}{\epsilon_{230}^{P1}} \quad Z_{P2} = \frac{\Delta S_{P2}}{\Delta S_{02}} \frac{\epsilon_{230}^{R2}}{\epsilon_{230}^{P2}} \tag{3}$$

In the following, we assumed that the ϵ at 230 nm of R1 and R2 and of their corresponding PPs within the same class are identical ($\epsilon_{230}^{X1} = \epsilon_{230}^{X2}$). Such an approximation is justified, at least for R1 and R2, by the fact that their absorption spectra are superimposable between 210 and 300 nm. The ϵ values used are derived from Johns et al. data (Table 2).[12]

The fractional amount of **1** and **2** and of their respective PPs as a function of the irradiation time is shown in Figure 3. The decay of TpT and the formation of its PPs in our experiment follow kinetics closely similar to the one reported by Johns et al.[12] upon 254 nm irradiation of TpT under comparable conditions. In particular, the c,s CPD PP increases up to $Z_{C2} = 0.225$ (Figure 3), compared to 0.210.[12] This fully justifies the use of TpT as an internal control to evaluate the photoreactivity of its 3′-*N*-sulfamate analogue TnsoT. Obviously, from Figure 3, it appears that R1 (TnsoT, **1**) is more photoreactive than R2 (TpT, **2**) as it decays faster and the initial rates of formation of the major R1-derived PPs are higher.

Quantum Yield Determination. The method that we developed determines the quantum yield of PP formation with respect to those obtained for TpT.[12] From extensive studies on TpT photochemistry, the simplest reaction scheme accounting for the formation of the primary TpT PPs can be written as

$$\text{P2} \xleftarrow{\Phi_{P2}} \text{R2} \underset{\Phi_{2-}}{\overset{\Phi_{C2}}{\rightleftharpoons}} \text{C2}$$

where Φ_{P2} and Φ_{C2} ($\Phi_{C2} = \Phi_{C2c,s} + \Phi_{C2t,s}$ I) are, respectively, the quantum yields for the formation of P2 (the (6-4) PP) and C2 (C2 = C2c,s + C2 trans-syn I (t,s I); the c,s CPD of **2** and the t,s I CPD isomer of **2** (**13**),[13] respectively). This reaction scheme is justified by the fact that Φ_{2-} (the CPD reversion yield) is identical for both the c,s and t,s I CPD isomers with the consequence that their molar ratio t,s I over c,s (whether originating from **1** (for C1t,s I, see structure **14**)[13] or **2**) remains practically constant (between 0.05 and 0.1) during the course of the photoreaction as initially observed by Johns et al.[12] The scheme above, however, is valid only for short irradiation times ($t \leq 5$ min) as secondary photoproducts such as the Dewar isomer of P2 will then accumulate.

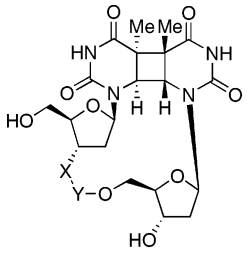

13 (C2t,s I) X=O, Y=PO_2^-

14 (C1t,s I) X=NH, Y=SO_2

The rate of formation, dP2/dt (mol min^{-1}), of P2 is given by eq 4:

$$\frac{\text{dP2}}{\text{d}t} = \Phi_{P2}(1 - 10^{-D})\text{IoS}\frac{D_{R2}}{D} \tag{4}$$

where D is the total optical density of the solution at 254 nm and D_{R2} is the corresponding optical density due to R2. The term $\text{IoS}(1 - 10^{-D})D_{R2}/D$ thus represents the 254 nm light dose rate (einsteins min^{-1}) absorbed by R2 at time t. For $t \leq 5$ min of the photoreaction, D remains sufficiently large ($D \geq 2$) so that the product $F = (1 - 10^{-D})\text{IoS}$ can be considered as a constant. This leads to eq 4′:

(12) Johns, H. E.; Pearson, M. L.; LeBlanc, J. C.; Helleiner, C. W. *J. Mol. Biol.* **1964**, *9*, 503−524.

(13) t,s I CPDs were tentatively identified from their retention time and UV spectrum. As they were minor compounds, they were not investigated further.

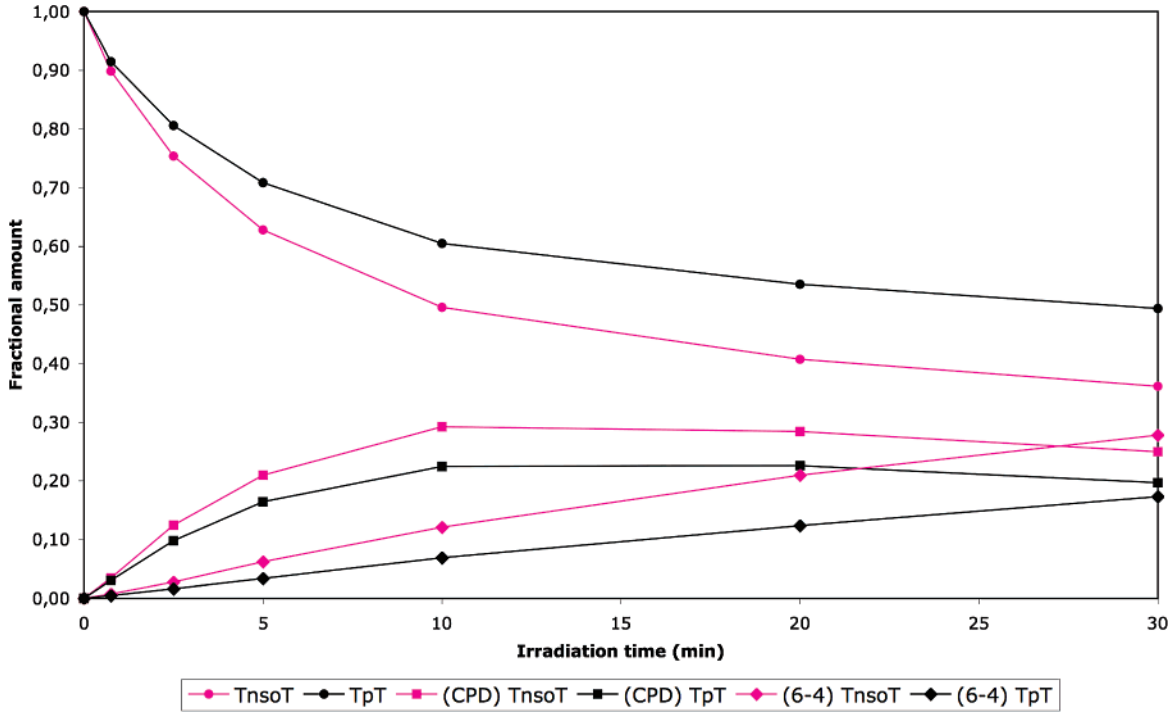

FIGURE 3. Fractional amount of the 3′-*N*-sulfamates TnsoT (**1**) and TpT (**2**) and of their respective photoproducts as a function of irradiation time.

$$\frac{\mathrm{dP2}}{\mathrm{d}t} = \Phi_{\mathrm{P2}} F \frac{D_{\mathrm{R2}}}{D} \qquad (4')$$

Taking into account the fact that D_{R1} and D_{R2} are the main components of D, eq 4′ can be integrated leading to a first approximation of eq 4″:

$$\mathrm{P2} = tF\Phi_{\mathrm{P2}} \frac{\overline{D_{\mathrm{R2}}}}{\bar{D}} \qquad (4'')$$

where $\overline{D_{\mathrm{R2}}}$ and $\bar{D}$ are the mean values of D_{R2} and D in the interval 0,t. Practically, $\overline{D_{\mathrm{R2}}}$ and $\bar{D}$ are the values of D_{R2} and D at t/2. The ratio of the quantum yields of formation of P2 and P1 is given by eq 4‴:

$$\frac{\Phi_{\mathrm{P1}}}{\Phi_{\mathrm{P2}}} = \frac{\mathrm{P1}}{\mathrm{P2}} \frac{\overline{D_{\mathrm{R2}}}}{\overline{D_{\mathrm{R1}}}} \qquad (4''')$$

The rate dC2/dt of formation of the CPDs of R2 is depicted by eq 5:

$$\frac{\mathrm{dC2}}{\mathrm{d}t} = F\left[\Phi_{\mathrm{C2}} \frac{D_{\mathrm{R2}}}{D} - \Phi_{2-} \frac{D_{\mathrm{C2}}}{D}\right] \qquad (5)$$

where D_{C2} refers to the 254 nm absorbance due to CPDs. At time $t^* \approx 10-15$ min, C2 reaches its maximal amount, C2* (Figure 3), and thus eq 5′ can be written as

$$\Phi_{\mathrm{C2}} D^*_{\mathrm{R2}} = \Phi_{2-} D^*_{\mathrm{C2}} \qquad (5')$$

leading finally to eq 5″:

$$\frac{\mathrm{dC2}}{\mathrm{d}t} = F\Phi_{\mathrm{C2}} \frac{D_{\mathrm{R2}}}{D}\left[1 - \frac{D^*_{\mathrm{R2}}}{D^*_{\mathrm{C2}}} \frac{D_{\mathrm{C2}}}{D_{\mathrm{R2}}}\right] \qquad (5'')$$

It should be noticed that because Φ_{2-} is identical for CPD isomers eqs 5, 5′, and 5″ remain valid for each CPD isomer.

The ratio $\Phi_{\mathrm{C1c,s}}/\Phi_{\mathrm{C2c,s}}$ is then obtained as described in the Experimental Section. The ratio of quantum yields and their absolute values taking the Φ values determined by Johns et al.[12] as reference yields are listed in Tables 3 and 4, respectively.

Consequently, the formation of both (6-4) PP and CPD is increased in the 3′-*N*-sulfamate series compared to TpT. Interestingly, the observed enhancement is significantly higher for the (6-4) PP than for the CPD PP (1.5 times).

Discussion

In dilute solutions, TnsoT (**1**) and TpT (**2**) are expected to adopt a large variety of conformations, whereas in their respective crystal structures, only one of these conformations is captured. Nevertheless, the data obtained so far indicate that characteristics observed in the solid state are generally representative of the major features observed in solution. For example, in the crystal structure of TnsoT reported here, the 5′- and 3′-sugars adopt a C3′-endo and C2′-endo puckering, respectively, in agreement with the NMR conformational analysis of **1** indicating that the 5′- and 3′-sugars exist in a major C3′-endo (69%) and a major C2′-endo (56%) conformation, respectively.[8b] Similarly, in the pTpT crystal structure,[14] both the 5′- and 3′-sugars are C2′-endo, the conformations that largely predominate at both ends in TpT in solution.[15] The observed

(14) Camerman, N.; Fawcett, J. K.; Camerman, A. *J. Mol. Biol.* **1976**, *107*, 601−621.
(15) Cheng, D. M.; Sarma, R. H. *J. Am. Chem. Soc.* **1977**, *99*, 7333−7348.

TABLE 3. Quantum Yield Ratios of PP Formation and CPD Reversion between the 3′-*N*-Sulfamate and the Natural Series

$\Phi_{C1c,s}/\Phi_{C2c,s}$	Φ_{P1}/Φ_{P2}	Φ_{1-}/Φ_{2-}
1.26 ± 0.08	1.8 ± 0.2	0.9 ± 0.1

TABLE 4. Quantum Yields of PP Formation and CPD Reversion in the Natural[12] and the 3′-*N*-Sulfamate Series

	Φ_P	$\Phi_{Cc,s}$	$\Phi-$
TpT[11]	10^{-3}	1.1 ± 10^{-2}	0.75
TnsoT	$(1.8 \pm 0.2)\ 10^{-3}$	$(1.38 \pm 0.06)\ 10^{-2}$	0.67 ± 0.08

conformational shift of the 5′-sugar toward C3′-endo puckering of **1** relative to **2** ($\Delta = 33\%$) has been attributed to a reduction in the gauche effect between the 3′-substituent and the O4′ atom, given that the 3′-amino group in **1** is less electronegative than the corresponding 3′-oxygen atom of **2**.[8b] On the other hand, circular dichroism data indicate that the estimated fraction of **1** present in solution in the stacked form is two times higher than that observed with **2**.[8b] In their respective crystal structures, intramolecular base stacking is clearly seen in **1** whereas in **2** the two bases are too far apart.

Thus, both crystal and solution data suggest that increasing the population of C3′-endo sugar puckering favors base stacking as was previously reported in the case of TmopTmo.[7] The stacking process could be mediated by the torsion angle ζ (C3′−N−S−O in the present case) which is driven by the sugar pucker-dependent torsion angle δ_A.[7] Hence, a C3′-endo conformation would lead to stacking whereas a C2′-endo conformation would lead to destacking. The crystal structure of **1** shows that both the C3′-endo conformation of the 5′-sugar and the g- conformation of ζ is associated with the stacked conformation. Interestingly, in the case of the pTpT crystal structure,[14] the reverse phenomenon is observed: the extended form, as a result of the trans conformation of the O3′−P bond, is associated with a C2′-endo puckering of the 5′-sugar. Consequently, it is likely that, in the phosphate and 3′-*N*-sulfamate series at least, only the 5′-sugar conformation is important for the stacking/destacking process.

The comparative irradiation experiment (Figure 3) shows that the initial rate of TnsoT (**1**) decay is roughly 1.35 times faster than that observed with TpT (**2**). This increased photoreactivity correlates with the higher propensity of **1** for base stacking than **2**. This is in line with our observations indicating that increasing the C3′-endo population of the sugar pucker of TpT by a chemical modification (2′-α-methoxylation or 3′-*N*-sulfamate analogue) results in an enhancement of base stacking and hence of the photoreactivity. In addition, the study herein indicates that the modification of the 5′-sugar conformation is sufficient to achieve this goal.

The relationship between the fraction of stacked species in **1** and **2** evaluated by circular dichroism (to be 2 times higher for **1** than for **2**) and the increased photoreactivity (1.35) is however not direct and should be more closely examined. Both **1** and **2** yielded the same types of photoproducts in solution, the CPD and (6-4) PP. Determination of their quantum yields of formation using **2** as a reference shows that both products form more efficiently from **1** than from **2** (Table 2). These results fully corroborate previous observations linking stacking ability and PP formation when temperature and solvent were varied.[16] In addition, the enhancement factor is significantly higher for the (6-4) PP than for the CPD (Table 3). A clue to further explore the relationship between stacking and photoreactivity is the crystal structure of **1** reported here. Examination of its stacking geometry (Figure 2) indicates that none of the sets of bonds involved in PP formation (C5−C6 of A and C5−C6 of B or C5−C6 of A and O4−C4 of B for the CPD or (6-4), respectively) are adequately positioned for a [2+2] cycloaddition to occur (even though these bonds are nearly parallel, they are too far in space (ca. 5.5 Å) for bond formation). This structure is thus typical of a stacked nonreactive conformation. Accordingly, the stacked fraction of **1** or **2** will comprise both nonproductive and minor photoreactive conformers. It can be concluded that the predominant C3′-endo sugar pucker at the 5′-end favors stacking but increases (6-4) PP formation more significantly than CPD formation. These data strongly suggest that distinct minor conformers lead, respectively, to the formation of (6-4) PPs and CPDs. The results obtained by the present study demonstrate that photochemistry is an efficient method to evidence the presence of minor but highly reactive conformations, whereas circular dichroism data reflect only average conformation properties.

The question that needs to be addressed at this stage is whether the ground-state minor active conformers are directly involved in the formation of the corresponding photoproducts. Excitation is fast (10^{-15} s),[17] and the first excited singlet state of thymine thought to be at the origin of CPD and (6-4) PP formation has a relatively short lifetime (10^{-12} s)[18] compared to the motion required to interconvert an active stacked conformer into either the corresponding unstacked form or another productive or nonproductive stacked form. Therefore, CPD and (6-4) PP formation is highly likely to derive essentially from the excitation of their corresponding minor active conformers. Clearly, the study of the dynamics of the stacked forms of **1** and **2** will help to clarify this point.

Interestingly, when the TpT sequence is embedded in an RNA duplex, its photoreactivity is dramatically reduced as compared to the one observed in B-DNA helix.[5b] This has been attributed to an increased rigidity of the double helix in the A conformation with respect to the B conformation which would preclude the prerequisite orientation for PP formation to occur. Indeed, in our context study, base pairing is absent as is the influence of neighboring nucleobases and these differences are likely to explain the different photochemical results.

Conclusion

Our results demonstrate that an increase of the C3′-endo sugar pucker of thymine dinucleotide analogues, through enhancement of the base stacking process, provokes an increased photoreactivity and an enhancement of PP quantum yields. The modification of the 5′-residue only appears to be sufficient to obtain the modification of the stacking status. Interestingly, the 3′-*N*-sulfamate backbone represents the first type of chemically modified dinucleotide analogue, reported so far, able to favor the (6-4) PP formation compared to the natural phosphate backbone. A search for modified thymine dinucleotide analogues leading to the selective and efficient (6-4) PP formation would

(16) (a) Hosszu, J. L.; Rahn, R. O. *Biochem. Biophys. Res. Commun.* **1967**, *29*, 327−330. (b) Wacker, A.; Lodemann, E. *Angew. Chem.* **1965**, *77*, 133. (c) Tramer, Z.; Wierzchowski, K. L.; Shugar, D. *Acta Biochim. Pol.* **1969**, *16*, 83−107.

(17) Turro, N. J. In *Molecular Photochemistry*; Breslow, R., Karplus, M., Eds.; Benjamin, W. A. Inc.: New York, 1967.

(18) Ruzsicska, B. P.; Lemaire, D. G. E. In *CRC Handbook of Organic Photochemistry and Photobiology*; Horspool, W. M., Song, P.-S., Eds.; CRC Press: Boca Raton, 1995; pp 1289−1317.

greatly facilitate the chemical synthesis of oligonucleotides containing (6-4) PP surrogates. Such compounds are steadily required for biological studies. In addition, **1** belongs to the promising 3′-*N*-sulfamate class of potential antisense and antigene agents. The report of its X-ray crystallographic structure should be helpful to the antisense and antigene chemist community.

Experimental Section

Irradiation Conditions. For analytical studies, an aqueous solution (1500 μL, HPLC grade) of compound **1** ($OD_{max} = 6.3$) or a 1:1 mixture of compounds **1** and **2** ($OD_{max} = 6.3$ for each solution) was prepared in a quartz cuvette (0.5 cm optical path). The oxygen of the solution was removed by argon bubbling for 30 min, and then the solution was exposed to the 254 nm light source (2 × 15 W, VL 215C Lamp, Vilber Lourmat, Marne la Vallée, France). An aliquot of the solution was sampled at $t = 0$, 0.75, 2.5, 5, 10, 20, and 30 min and analyzed by reversed-phase HPLC. For preparative purposes, an aqueous solution of **6** (115 mg in 230 mL) was exposed for 2 h to the 254 nm light (12 × 8 W; T8C UVC 7H 8W Lamps, Vilber Lourmat, Marne la Vallée, France). The photolysate was concentrated to dryness and purified by reversed-phase HPLC.

HPLC Conditions. Analytic HPLC. A portion of 25 μL of the irradiation mixture was injected on a SYMMETRY C18 (5 μm, 4.6 × 250 mm) column using a 50 min, 1 mL/min gradient of 0−15%, then 5 min of 15−20% CH_3CN in 0.05 M aqueous ammonium acetate. A photodiode array detector was used. Peak areas were measured at 230 nm. Retention time (min): TnsoT series, (6-4) PP **7** 17.6, CPD PP **8** 21.4, TnsoT **1** 42.1; TpT series, CPD PP **12** 7.1, (6-4) PP **11** 10.1, TpT **2** 28.1.

Preparative HPLC. Preparative purification was performed on an Hypersil HSC18 (5 μm, 100 Å, 21.2 × 250 mm) column using a 45 min, 12 mL/min linear gradient of 0−25% CH_3CN in H_2O. The detection was set at 230 nm. The (6-4) PP **9** (22 mg, 19%), the CPD PP **10** (12 mg, 10%), and the recovered starting material **6** (32 mg, 22%) were obtained after evaporation of the appropriate fractions. Retention time (min): (6-4) PP **9**, 31; CPD PP **10**, 46; compound **6**, 50.

Chemical Correlation between PPs of 6 and 2. An aqueous solution of a 1:1 mixture of compounds **6** and **2** ($OD_{max} = 6.3$ for each solution) was exposed for 10 min to the 254 nm light source. An aliquot of the solution was analyzed by HPLC. Then TEA was added to the photolysate, and the mixture was stirred for 5 min. An aliquot of the solution was analyzed by HPLC.

Quantum Yield Determination. Quantum yields were determined using the assumption that $\epsilon^{X1} = \epsilon^{X2}$ at both 230 and 254 nm. The ratios can then be expressed directly from experimental data.

$$\frac{\Phi_{P1}}{\Phi_{P2}} = \frac{\Delta S_{P1}}{\Delta S_{P2}} \frac{\overline{\Delta S_{R2}}}{\overline{\Delta S_{R1}}} \quad (1)$$

$$\frac{\Phi_{C1}}{\Phi_{C2}} = \frac{\Delta S_{C1}}{\Delta S_{C2}} \frac{\overline{\Delta S_{R2}}}{\overline{\Delta S_{R1}}} \frac{\rho 2}{\rho 1} \text{ with } \rho 2 = 1 - \frac{\Delta S^*_{R2}}{\Delta S^*_{C2}} \frac{\overline{\Delta S_{C2}}}{\overline{\Delta S_{R2}}} \text{ and}$$

$$\rho 1 = 1 - \frac{\Delta S^*_{R1}}{\Delta S^*_{C1}} \frac{\overline{\Delta S_{C1}}}{\overline{\Delta S_{R1}}} \quad (2)$$

$$\frac{\Phi_{1-}}{\Phi_{2-}} = \frac{\Phi_{C1}}{\Phi_{C2}} \frac{\Delta S^*_{R1}}{\Delta S^*_{C1}} \frac{\Delta S^*_{C2}}{\Delta S^*_{R2}} \text{ where } \overline{\Delta S_{R2}} = \Delta S_{R2} \text{ measured at } t/2 \quad (3)$$

As discussed in the Results, eqs 2 and 3 can be applied to c,s CPD, t,s I CPD, or their sum.

3′-Deoxythymidin-3′-ylsulfamoyl-[3′(*N*)->5′(*O*)]-thymidine 1. 4-Nitrophenyl 5′-*O*-(4,4′-dimethoxytrityl)-3′-deoxythymidine-3′-sulfamate **3**[8b] (697 mg, 0.93 mmol) was condensed to 3′-*O*-acetylthymidine **4** (500 mg, 1.76 mmol) according to the published procedure.[8b] The dimer intermediate **5** (566 mg) was obtained in 68% yield. This intermediate (176 mg, 0.19 mmol) was deacetylated in a mixture of MeOH/TEA/H_2O (8:1:1) (10 mL) for 20 h at room temperature and then for 4 h at 50 °C and then concentrated to dryness. The residue was solubilized in CH_2Cl_2 (3 mL). Then 80% aqueous acetic acid (5 mL) was added, and the mixture was stirred at room temperature for 3 h. The reaction mixture was diluted with H_2O (30 mL). The aqueous phase was washed with CH_2Cl_2 (30 mL), concentrated, and purified by reversed-phase chromatography (LiChroprep RP-18) using a gradient of CH_3CN in H_2O (0−20%) to give **1**[8b] in 82% yield (two steps).

3′-Deoxythymidin-3′-ylsulfamoyl-[3′(*N*)->5′(*O*)]-3′-*O*-acetylthymidine 6. To the dimer intermediate **5** (440 mg, 0.49 mmol) was added a solution of 3% CF_3COOH in CH_2Cl_2 (40 mL). The reaction was stirred for 10 min at room temperature, and then MeOH was added. The solvants were evaporated to give a residue that was purified by silica gel chromatography using a gradient of MeOH in CH_2Cl_2 (0−10%) give **6** in 92% yield (266 mg). ^{1}H NMR (600 MHz, D_2O): δ 1.91 (3H, s, CH_3-5 pT), 1.92 (3H, s, CH_3-5 Tp), 2.19 (3H, s, CO*CH*$_3$), 2.47−2.56 (2H, m, H-2′ and H-2″Tp), 2.50−2.60 (2H, m, H-2′ and H-2″ pT), 3.84 (1H, dd, $J = 13.0$, 3.7 Hz, H-5′ Tp), 3.96 (1H, dd, $J = 13.0$, 2.5 Hz, H-5″ Tp), 4.04−4.10 (2H, m, H-3′ and H-4′ Tp), 4.45−4.51 (3H, m, H-4′, H-5′ and H-5″ pT), 5.43 (1H, ddd, $J = 6.8$, 3.4, 3.4 Hz, H-3′ pT), 6.13 (1H, dd, $J = 6.8$, 4.9 Hz, H-1′ Tp), 6.37 (1H, dd, $J = 7.0$, 7.0 Hz, H-1′ pT), 7.62 (1H, s, H-6 pT), 7.75 (1H, s, H-6 Tp). IR (film, cm^{-1}) 3410, 3207, 3066, 1692, 1467, 1361, 1238, 1172, 1097, 1044, 957. HRMS (ES) $(M + Na)^+$ calcd for $C_{22}H_{29}N_5O_{12}NaS$, 610.1431; found, 610.1456.

Cyclobutane Photoproduct 10. ^{1}H NMR (600 MHz, D_2O): δ 1.48 (3H, s, CH_3-5 pT), 1.59 (3H, s, CH_3-5 Tp), 2.12 (3H, s, CO*CH*$_3$), 2.25 (1H, br ddd, $J = 14.4$, 7.8, 7.2 Hz, H-2″ Tp), 2.29 (1H, ddd, $J = 13.9$, 4.8, 1.6 Hz, H-2″ pT), 2.51 (1H, ddd, $J = 13.9$, 10.3, 7.3 Hz, H-2′ pT), 3.00 (1H, ddd, $J = 14.4$, 7.2, 5.2 Hz, H-2′ Tp), 3.75 (1H, dd, $J = 13.6$, 2.9 Hz, H-5′ Tp), 3.85 (1H, ddd, $J = 13.6$, 3.6 Hz, H-5″ Tp), 3.94 (1H, ddd, $J = 6.2$, 3.5, 2.9 Hz, H-4′ Tp), 4.00 (1H, ddd, $J = 7.8$, 7.2, 6.2 Hz, H-3′ Tp), 4.30 (1H, m, H-4′ pT), 4.37 (1H, d, $J = 6.4$ Hz, H-6 Tp), 4.44−4.49 (2H, m, H-5′ and H-5" pT), 4.57 (1H, d, $J = 6.4$ Hz, H-6 pT), 5.29 (1H, ddd, $J = 7.3$, 3.2, 1.6 Hz, H-3′ pT), 5.93 (1H, dd, $J = 10.3$, 4.8 Hz, H-1′ pT), 5.96 (1H, br dd, $J = 7.2$, 5.2 Hz, H-1′ Tp). ^{13}C NMR (150 MHz, D_2O): δ 17.8 (CH_3 pT), 18.1 (CH_3 Tp), 21.5 (CO*CH*$_3$), 34.0 (C-2′ Tp), 35.0 (C-2′ pT), 47.0 and 54.2 (C-5 Tp and pT), 53.5 (C-3′ Tp), 56.5 (C-6 pT), 60.6 (C-6 Tp), 61.1 (C-5′ Tp), 70.6 (C-5′ pT), 73.6 (C-3′ pT), 80.7 (C-4′ pT), 82.4 (C-4′ Tp), 86.9 (C-1′ Tp), 87.5 (C-1′ pT), 155.5 (C-2 Tp), 156.1 (C-2 pT), 172.8 (C-4 Tp), 174.8 (*CO*CH$_3$), 175.3 (C-4 pT). IR (film, cm^{-1}) 3427, 3233, 3075, 1705, 1454, 1366, 1282, 1207, 1177, 1089, 1036, 952. HRMS (ES) $(M + Na)^+$ calcd for $C_{22}H_{29}N_5O_{12}NaS$, 610.1431; found, 610.1426.

(6-4) Photoproduct 9. ^{1}H NMR (600 MHz, D_2O): δ 1.49 (1H, ddd, $J = 13.9$, 6.7, 1.0 Hz, H-2′ Tp), 1.77 (3H, s, CH_3-5 Tp), 2.08 (1H, ddd, $J = 13.9$, 13.1, 8.4 Hz, H-2″ Tp), 2.16 (3H, s, CO*CH*$_3$), 2.35 (3H, s, CH_3-5 pT), 2.86 (1H, ddd, $J = 15.4$, 8.0, 7.2 Hz, H-2″ pT), 3.16 (1H, ddd, $J = 15.4$, 7.4, 2.5 Hz, H-2′ pT), 3.24 (1H, ddd, $J = 13.1$, 9.9, 6.7 Hz, H-3′ Tp), 3.30 (1H, ddd, $J = 9.9$, 3.2, 2.3 Hz, H-4′ Tp), 3.82 (1H, dd, $J = 13.1$, 3.2 Hz, H-5′ Tp), 4.01 (1H, dd, $J = 13.1$, 2.3 Hz, H-5′ Tp), 4.04 (1H, dd, $J = 11.3$, 2.0 Hz, H-5′ pT), 4.47 (1H, dd, $J = 11.3$, 1.4 Hz, H-5′ pT), 4.49 (1H, m, H-4′ pT), 5.22 (1H, s, H-6 Tp), 5.67 (1H, ddd, $J = 7.4$, 7.2, 4.2 Hz, H-3′ pT), 6.23 (1H, dd, $J = 8.4$, 1.0 Hz, H-1′ Tp), 6.59 (1H, dd, $J = 8.0$, 2.5 Hz, H-1′ pT), 8.08 (1H, s, H-6 pT). ^{13}C NMR

(150 MHz, D_2O): δ 14.9 (CH_3 pT), 21.4 (CO*CH3*), 26.3 (CH3 Tp), 33.7 (C-2′ pT), 35.2 (C-2′ Tp), 51.0 (C-3′ Tp), 59.0 (C-5′ Tp), 59.3 (C-6 Tp), 71.5 (C-5′ pT), 73.7 (C-3′ pT), 74.4 (C-5 Tp), 83.4 (C-1′ Tp and C-4′ Tp), 83.9 (C-4′ pT), 89.5 (C-1′ pT), 117.9 (C-5 pT), 155.1 (C-2 Tp), 158.4 (C-2 pT), 174.9 (*CO*CH_3), 175.2 (C-4 Tp), 176.0 (C-4 pT). IR (film, cm^{-1}) 3401, 3242, 3110, 1723, 1687, 1652, 1507, 1450, 1366, 1243, 1177, 1102, 1053, 939. HRMS (ES) $(M + Na)^+$ calcd for $C_{22}H_{29}N_5O_{12}NaS$, 610.1431; found, 610.1449.

Acknowledgment. We thank Dr. Daniel Royer for recording IR spectra.

Supporting Information Available: General information, chromatograms of the irradiation of **1** + **2**, NMR spectra of compound **1** irradiation, compounds **6**, **9**, and **10**, and X-ray crystallographic data for **1** (in CIF format). This material is available free of charge via the Internet at http://pubs.acs.org.

JO061488A